Improved bipartition model of electron transport. I. A general formulation

Luo Zheng-ming*
Institut für Medizinische Strahlenkunde der Universität Würzburg, D-8700 Würzburg, Federal Republic of Germany
(Received 2 October 1984)

In an earlier paper [Radiat. Res. **92**, 1 (1982)], a bipartition model of electron transport has been proposed. In this model an electron beam is divided into two components: one describing the penetration of the small-angle scattered electrons, another describing the diffusion of electrons that have undergone large-angle scattering. In the present work, which consists of a series of three articles (the third to appear at a later date), the bipartition model of electron transport is refined and is applied to problems that include electron transport in inhomogeneous media and discrete energy-loss processes. In the present paper (the first one in the series), the treatment is restricted to the application of the continuous-slowing-down approximation model to homogeneous media and to comparisons of the results with Spencer's moment method and with experimental data. The comparisons show that the improved and more flexible bipartition model has high precision.

I. INTRODUCTION

Transport problems of electrons and charged particles are attracting increasing attention. While they remain important in nuclear physics, in radiation measurements, and in radiation dosimetry, they are, by now essential also in a variety of other fields of research. Transport problems of electrons and other charged particles are relevant, for example, to the interaction between the fusion plasma and the first wall of fusion reactors, the fusion process induced by laser beams or relativistic electron beam, the technology of electron or ion beams, or the ion-beam modification of materials. Such applications make it desirable to develop new theories of electron and charged particle transport that possess higher precision and more versatility.[1]

In the past the Monte Carlo method has been most extensively used for different transport problems of electrons and charged particles.[2–10] The main advantage of the Monte Carlo method is flexibility; in principle, and as far as the interactions and their cross sections between electrons and matter are known, the method can be applied to simulate electron transport even for complex geometries. However, the Monte Carlo method has limitations. One of these is the problem of statistical errors and the resultant need for a large number of repeated calculations to reach adequate precision of the results. If one is interested in events with small probability, for example, if one wants to calculate electron fluence differential in energy and angle at specified points in a medium, it can be difficult to find adequate sampling methods. Generally, Monte Carlo computations can be inefficient if solutions throughout space have to be determined for extended, inhomogeneous sources.

Analytical methods are an important alternative for electron-transport calculations. In the case of thin foils, several analytical approaches have been developed and have been applied towards the investigation of the angular distributions and the energy-loss distributions of electrons that penetrate such foils.[11–25] The applicability of the analytical theories to deep penetration of electrons into matter has been much more restricted. Spencer's moment method has been the most important and the most effective treatment of the transport of electrons in homogeneous media.[26–30] It is, however, difficult to extend Spencer's method to inhomogeneous media. Analytical theories based on the spherical harmonic expansion with lower-order approximations or on the Fokker-Planck approximation have been developed by Bethe *et al.*; they are comparatively simple but they are of approximate nature and their accuracy is not satisfactory for many-electron-transport problems.[31–35] An alternative is the discrete ordinates methods that has been applied successfully in recent years towards the solution of various electron-transport problems.[36] There remains, however, a need for improved analytical methods with higher accuracy and with sufficient flexibility to accommodate a wider range of electron-transport problems.

In 1967 another analytical theory, a bipartition model of electron transport, was presented.[1] The main idea of the theory is the separation of the electron beam into two components. Since the theoretical treatment of small-angle scattering cannot be applied to the transport of electrons undergoing large-angle scattering, by means of a partition condition mentioned later, the large-angle scattered electrons are separated from the small-angle scattered electrons and are followed separately. They are called the diffusion-electron group, and their transport is analyzed in terms of the Pn approximation. The small-angle scattered electrons are called the straightforward-electron group and their transport is treated in terms of the familiar small-angle approximation. A demonstration of the separation of the electron beam has been shown in the Fig. 1. The earlier computations of electron-energy deposition have demonstrated good accuracy of the bipartition model and its applicability to transport problems of electrons in inhomogeneous media. The present work has now led to improvements both in the treatment of the

diffusion-electron group and the straightforward-electron group. The angular distribution of the diffusion-electron group is more accurately described and a higher-order expansion of spherical harmonic polynomials is utilized for the description of its transport. The small-angle scattering of the straightforward-electron group is treated more rigorously, and a better description of the attenuation process of these electrons is achieved. Apart from these improvements, the applicability of the bipartition model has been extended and is now used for the treatment of electron transport in inhomogeneous media. For example, oblique incidence of an electron beam into a semiinfinite or a multilayer medium is considered, and the energy-loss straggling of electrons in thick media is treated. These applications are the objective of the two subsequent articles. The present article is concerned with the application of the continuous-slowing-down (CSD) approximation to homogeneous media and to a comparison with Spencer's calculations and experimental results.

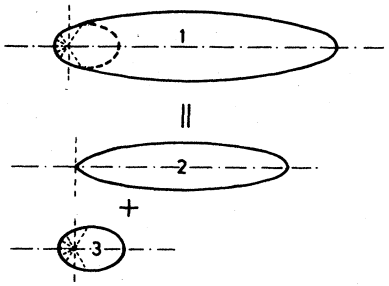

FIG. 1. Demonstration of the bipartition of an electron beam. Passing through a certain thickness of a medium the angular distribution of the straightforward electrons, which is marked by part 1 of this figure, is broadened. By means of the partition condition the broadened angular distribution is divided into two parts. The part surrounded by the thick-dashed lines in part 1 is regarded as a diffusion electron source and is also shown in part 3. The thin-dashed lines represent the large-angle direction selected. The rest part still belongs to the straightforward electrons and is shown in part 2.

II. THE TRANSPORT EQUATIONS OF ELECTRON

In Ref. 37, a transport equation of electrons, that takes into account the accumulation of secondary δ electrons, was presented and used to analyze the cavity ionization phenomenon. In the present work, this electron-transport equation is used as a starting point and is then simplified by successive approximations.

The electron-transport equation neglecting bremsstrahlung but taking into account the buildup of the secondary δ electrons is

$$\begin{aligned}\mathbf{u}\cdot\nabla f(\mathbf{r},\mathbf{u},E)=&\int_{4\pi}[f(\mathbf{r},\mathbf{u}',E)-f(\mathbf{r},\mathbf{u},E)]\frac{N_A}{A}\sigma_N(E,\mathbf{u}\cdot\mathbf{u}')d\mathbf{u}'\\&+\int_E^{E_0}\int_{4\pi}f(\mathbf{r},\mathbf{u}',E')\frac{N_A}{2\pi A}Z\sigma_M(E',E'-E)\delta[\mathbf{u}\cdot\mathbf{u}'-\varphi(E',E)]dE'\,d\mathbf{u}'\\&-f(\mathbf{r},\mathbf{u},E)\int_0^{E/2}\int_{4\pi}\frac{N_A}{2\pi A}Z\sigma_M(E,\tau)\delta(\mathbf{u},\mathbf{u}'-\varphi)d\tau\,d\mathbf{u}'+S(\mathbf{r},\mathbf{u},E)\,,\end{aligned}\tag{1}$$

where

$$\varphi(E',E)=\frac{1}{2}\left[\left[\frac{E(2+E)}{(E'-E)(2+E'-E)}\right]^{1/2}+\left[\frac{(E'-E)(2+E'-E)}{E(2+E)}\right]^{1/2}-\left[\frac{E'^2(2+E')^2}{E(2+E)(E'-E)(2+E'-E)}\right]^{1/2}\right].\tag{2}$$

$f(\mathbf{r},\mathbf{u},E)$ is the electron fluence differential in angle and energy, i.e., $f(\mathbf{r},\mathbf{u},E)d\mathbf{u}\,dE$ is the fluence of electron at the point $\mathbf{r}$, with directions between $\mathbf{u}$ and $\mathbf{u}+d\mathbf{u}$ and with energy between E and $E+dE$. σ_N is the differential elastic scattering cross section of electrons in the Coulomb field of the nucleus. σ_M is Möller cross section of electron-electron scattering, and N_A is the Avogadro number. E_0 is the maximum electron energy of the source. It is difficult to solve Eq. (1) directly, because of the predominance of the small-angle scattering with small energy transfer. The ordinary two-dimensional expansion would, therefore, be very long and tedious. Accordingly, certain realistic simplifications need to be made in Eq. (1).

Let C_{in} be the inelastic scattering term of electron in Eq. (1), i.e.,

$$\begin{aligned}C_{\text{in}}=&\int_E^{E_0}\int_{4\pi}f(\mathbf{r},\mathbf{u}',E')\frac{N_A}{2\pi A}Z\sigma_M\delta(\mathbf{u}\cdot\mathbf{u}'-\varphi)dE'\,d\mathbf{u}'-f(\mathbf{r},\mathbf{u},E)\int_0^{E/2}\frac{N_A}{A}Z\sigma_M(E,\tau)d\tau\\=&\int_E^{E_0}f(\mathbf{r},\mathbf{u},E')\frac{N_A}{A}Z\sigma_M(E',E'-E)dE'-f(\mathbf{r},\mathbf{u},E)\int_0^{E/2}\frac{N_A}{A}Z\sigma_M(E,\tau)d\tau+C'_{\text{in}}\,.\end{aligned}\tag{3}$$

Here, C'_{in} is

$$C'_{\text{in}}=\int_E^{E_0}\int_{4\pi}[f(\mathbf{r},\mathbf{u}',E')-f(\mathbf{r},\mathbf{u},E')]\frac{N_A}{2\pi A}Z\sigma_M(E',E'-E)\delta[\mathbf{u}\cdot\mathbf{u}'-\varphi(E',E)]dE'\,d\mathbf{u}'\,.\tag{4}$$

Expanding the function under the integral sign in Eq. (4) to the second order around E, we have

$$C'_{\text{in}} \approx \int_{4\pi}[f(\mathbf{r},\mathbf{u}',E)-f(\mathbf{r},\mathbf{u},E)]\frac{N_A}{A}Z\sigma_e(E,\mathbf{u}\cdot\mathbf{u}')d\mathbf{u}'+\frac{d}{dE}\int[f(\mathbf{r},\mathbf{u},E)-f(\mathbf{r},\mathbf{u},E)]\frac{N_A}{2\pi A}Z\rho_e(E,\mathbf{u}\cdot\mathbf{u}')d\mathbf{u}' \tag{5}$$

and

$$\rho_e(E,\mathbf{u}\cdot\mathbf{u}')=\int_0^{E/2}\sigma_M(E,\tau)\tau\delta[\mathbf{u}\cdot\mathbf{u}'-\varphi(E,\tau)]d\tau\ . \tag{6}$$

Neglecting the term containing $\rho_e(E,\mathbf{u}\cdot\mathbf{u}')$, we have the first approximation for the electron-transport equation

$$\begin{aligned}\mathbf{u}\cdot\nabla f(\mathbf{r},\mathbf{u},E)=&\int_{4\pi}[f(\mathbf{r},\mathbf{u}',E)-f(\mathbf{r},\mathbf{u},E)]\frac{N_A}{A}(\sigma_N+Z\sigma_e)d\mathbf{u}'\\&+\int_E^{E_0}f(\mathbf{r},\mathbf{u},E')\frac{N_A}{A}Z\sigma_M(E',E'-E)dE'-\int_0^{E/2}f(\mathbf{r},\mathbf{u},E)\frac{N_A}{A}Z\sigma_M(E,\tau)d\tau+S(\mathbf{r},\mathbf{u},E)\ .\end{aligned} \tag{7}$$

This approximation amounts to disregarding the correlation between small energy transfers and small-angle deflections. There is no contribution of secondary electrons to the fluence in the energy interval between $[E_0,E_0/2]$, accordingly the integral term of the energy transfer can be divided into two parts. One part is

$$\int_E^{2E}f(\mathbf{r},\mathbf{u},E')\frac{N_AZ}{A}\sigma_M(E',E'-E)dE'\ . \tag{8}$$

It represents the change of electrons with energy E' into electrons with lower energy E due to energy losses. The other part is

$$\int_{2E}^{E_0}f(\mathbf{r},\mathbf{u},E')\frac{N_AZ}{A}\sigma_M(E',E'-E)dE'\ . \tag{9}$$

This term represents the secondary δ electrons generated by the electrons with energy E'. Applying Eq. (7) to thin layer and neglecting the term of scattering lead to Landau's dynamic equation. Accordingly for thick layers the Fokker-Planck approximation can also be valid. Expanding the functions under the integral sign in Eq. (7) to second order around E, we have a transport equation that takes into account the buildup of the secondary electrons within the Fokker-Planck approximation:

$$\begin{aligned}\mathbf{u}\cdot\nabla f(\mathbf{r},\mathbf{u},E)=&\frac{\partial f\rho}{\partial E}+\frac{1}{2}\frac{\partial^2 f\Omega}{\partial E^2}+\int_{2E}^{E_0}f(\mathbf{r},\mathbf{u},E')\frac{N_A}{A}Z\sigma_M(E',E'-E)dE'\\&+\int_{4\pi}[f(\mathbf{r},\mathbf{u}',E)-f(\mathbf{r},\mathbf{u},E)]\frac{N_A}{A}(\sigma_N+Z\sigma_e)d\mathbf{u}'+S(\mathbf{r},\mathbf{u},E)\ ,\end{aligned} \tag{10}$$

$$\rho(E)=\int_0^{E/2}\tau\frac{N_A}{A}Z\sigma_M(E,\tau)d\tau,\quad \Omega(E)=\int_0^{E/2}\tau^2\frac{N_A}{A}Z\sigma_M(E,\tau)d\tau\ .$$

Neglecting the buildup of secondary δ electrons, we have

$$\mathbf{u}\cdot\nabla f(\mathbf{r},\mathbf{u},E)=\frac{\partial f\rho}{\partial E}+\frac{1}{2}\frac{\partial^2 f\Omega}{\partial E^2}+\int_{4\pi}[f(\mathbf{r},\mathbf{u}',E)-f(\mathbf{r},\mathbf{u},E)]\frac{N_A}{A}(\sigma_N+Z\sigma_e)d\mathbf{u}'+S(\mathbf{r},\mathbf{u},E)\ . \tag{11}$$

In order to obtain the Lewis electron-transport equation in the continuous-slowing-down approximation (CSDA) model, one can neglect the second order differential term in Eq. (11) and introduce the following transformation:

$$t=1-\frac{1}{R_0}\int_E^{E_0}\left[\frac{dE'}{dx}\right]^{-1}dE'\ , \tag{12}$$

$$f(\mathbf{r},\mathbf{u},E)=f(\mathbf{r},\mathbf{u},t)\left[\frac{dE}{dx}\right]^{-1}\Big/R_0,\quad S(\mathbf{r},\mathbf{u},E)=S(\mathbf{r},\mathbf{u},t)\left[\frac{dE}{dx}\right]^{-1}\Big/R_0\ . \tag{13}$$

Therefore, we have

$$\mathbf{u}\cdot\nabla f(\mathbf{r},\mathbf{u},t)=\frac{\partial f(\mathbf{r},\mathbf{u},t)}{\partial t}+\int_{4\pi}\frac{N_A}{A}R_0(\sigma_N+Z\sigma_e)[f(\mathbf{r},\mathbf{u}',t)-f(\mathbf{r},\mathbf{u},t)]d\mathbf{u}'+S(\mathbf{r},\mathbf{u},t)\ , \tag{14}$$

where R_0 is the range of electrons with initial energy E_0 and (dE/dx) is the stopping power. Now several integral formulas can be introduced. Let $F_0(E)$ be

$$F_0(E)=\int_V\int_{4\pi}f(\mathbf{r},\mathbf{u},E)d\mathbf{u}\,d\mathbf{r}\ . \tag{15}$$

For Eq. (7) we have

$$\begin{aligned}\int_E^{2E}dE'\,F_0(E')\int_{E'-E}^{E'/2}\sigma_M(E',\tau)&=\int_{2E}^{E_0}dE'\,F_0(E')\int_E^{E'/2}\sigma_M(E',\tau)d\tau\\&\quad+\int_E^{E_0}S_0(E')dE'\ ,\end{aligned} \tag{16}$$

$$\int_E^{E_0} F_0(E')dE' \int_0^E \tau\sigma_M(E',\tau)d\tau = \int_E^{E_0} E'S_0(E')dE' , \tag{17}$$

where

$$S_0(E) = \int_V \int_{4\pi} S(\mathbf{r},\mathbf{u},E)d\mathbf{u}\,d\mathbf{r} . \tag{18}$$

For Eq. (11) we have

$$\frac{d\rho F_0(E)}{dE} + \frac{1}{2}\frac{d^2}{dE^2}[F_0(E)\Omega(E)] = S_0(E) , \tag{19}$$

then

$$F_0(E)\rho(E) + \frac{1}{2}\frac{dF_0\Omega}{dE} = \int_E^{E_0} S_0(E')dE' , \tag{20}$$

and when $E \to 0$, we have

$$\int_E^{E_0} F_0(E')\rho(E')dE' = \int_E^{E_0} E'S_0(E')dE' . \tag{21}$$

Equations (17) and (16) represent the conservation laws of electron number and electron energy. The integral formulas have been utilized to assess the accuracy of the numerical computations.

III. A BIPARTITION SOLUTION OF LEWIS TRANSPORT EQUATION

It is assumed that a monoenergetic and monodirectional plane electron source is embedded in an infinite homogeneous medium, and that the emission direction of the source is parallel to the normal of the plane. Let the initial energy of electrons be E_0 and choose an x axis in the emission direction, with the origin on the source plane. The Lewis electron-transport equation is then

$$-\frac{\partial f}{\partial t} + \mu\frac{\partial f}{\partial x} = \int_{4\pi} \frac{N_A R_0}{A}\sigma(t,\mathbf{u}\cdot\mathbf{u}') \times [f(x,\mu',t) - f(x,\mu,t)]d\mathbf{u}' + \frac{1}{2\pi}\delta(1-\mu)\delta(1-t)\delta(x) , \tag{22}$$

where $\mu = \cos\theta$, θ is the angle between the direction of electron motion and the x axis. σ is the total differential cross section of the scattering of the nucleus and the electrons in the atom. We introduce the following solution of Eq. (22):

$$f(x,\mu,t) = f_s(x,\mu,t) + f_d(x,\mu,t) , \tag{23}$$

where $f_s(x,\mu,t)$ is the fluence differential in μ and t of the straightforward electrons, while $f_d(x,\mu,t)$ is the corresponding fluence for the diffusion electrons. According to Ref. 1 we may divide the equation (22) into two parts

$$-\frac{\partial f_s}{\partial t} + \mu\frac{\partial f_s}{\partial x} = \int_{4\pi} \frac{N_A R_0}{A}\sigma(t,\mathbf{u}\cdot\mathbf{u}')[f_s(x,\mu',t) - f_s(x,\mu,t)]d\mathbf{u}' - S_{\text{diff}}(x,\mu,t) + \frac{1}{2\pi}\delta(1-\mu)\delta(1-t)\delta(x) \tag{24}$$

and

$$-\frac{\partial f_d}{\partial t} + \mu\frac{\partial f_d}{\partial x} = \int_{4\pi} \frac{N_A R_0}{A}\sigma(t,\mathbf{u}\cdot\mathbf{u}')[f_d(x,\mu',t) - f_d(x,\mu,t)]d\mathbf{u}' + S_{\text{diff}}(x,\mu,t) . \tag{25}$$

Expanding $f_s(x,\mu,t)$, $f_d(x,\mu,t)$, $S_{\text{diff}}(x,\mu,t)$ into the series of the spherical harmonic functions, we have

$$f_s(x,\mu,t) = \sum_{l=0}^{\infty} \frac{2l+1}{4\pi} P_l(\mu)A_l(t,x) , \tag{26}$$

$$f_d(x,\mu,t) = \sum_{l=0}^{\infty} \frac{2l+1}{4\pi} P_l(\mu)N_l(t,x) , \tag{27}$$

$$S_{\text{diff}}(x,\mu,t) = \sum_{l=0}^{m} \frac{2l+1}{4\pi} P_l(\mu)S_l(t,x) . \tag{28}$$

The choice of the integer m depends on the desired computational precision, where

$$A_l(t,x) = 2\pi \int_{-1}^{1} P_l(\mu)f_s(x,\mu,t)d\mu , \tag{29}$$

$$N_l(t,x) = 2\pi \int_{-1}^{1} P_l(\mu)f_d(x,\mu,t)d\mu , \tag{30}$$

$$S_l(t,x) = 2\pi \int_{-1}^{1} P_l(\mu)S_{\text{diff}}(x,\mu,t)d\mu . \tag{31}$$

Let C_f express the scattering integral term in the transport equation, i.e.,

$$C_f = \int_{4\pi} \frac{N_A R_0}{A}\sigma(t,\boldsymbol{\mu}\cdot\boldsymbol{\mu}')[f_s(x,\mu',t) - f_s(x,\mu,t)]d\mathbf{u}' . \tag{32}$$

By using Blanchard's and Spencer's approximation formulas,[38] we have

$$C_f=-\sum_{n=0}^{\infty}\frac{2n+1}{4\pi}P_n(\mu)A_n(t,x)\frac{\alpha d_n}{t(t+\alpha)}\ , \tag{33}$$

where α and d_n are constants. We introduce the partition condition

$$S_{\text{diff}}(x,\mu_i,t)=C_f(x,\mu_i,t),\quad i=0,1,\cdots,m\ . \tag{34}$$

Equation (34) can be written in detail as the following linear system:

$$\begin{bmatrix} 1 & \mu_0 & \cdots & P_l(\mu_0) & \cdots & P_m(\mu_0) \\ 1 & \mu_1 & \cdots & P_l(\mu_1) & \cdots & P_m(\mu_1) \\ \vdots & \vdots & & \vdots & & \vdots \\ 1 & \mu_m & \cdots & P_l(\mu_m) & \cdots & P_m(\mu_m) \end{bmatrix} \begin{bmatrix} S_0 \\ 3S_1 \\ \vdots \\ (2m+1)S_m \end{bmatrix} = 4\pi \begin{bmatrix} C_f(\mu_0) \\ C_f(\mu_1) \\ \vdots \\ C_f(\mu_m) \end{bmatrix} .$$

Thus,

$$S_l(t,x)=-\sum_{n=0}^{\infty}D_{nl}\frac{\alpha d_n}{t(t+\alpha)}A_n(t,x)\ ,$$

$$D_{nl}=\frac{2n+1}{2l+1}\ \frac{\begin{bmatrix} 1 & \mu_0 & \cdots & P_{l-1}(\mu_0), & P_n(\mu_0), & P_{l+1}(\mu_0), & \cdots & P_m(\mu_0) \\ 1 & \mu_1 & \cdots & P_{l-1}(\mu_1), & P_n(\mu_1), & P_{l+1}(\mu_1), & \cdots & P_n(\mu_1) \\ \vdots & \vdots & \cdots & \vdots & \vdots & \vdots & & \vdots \\ 1 & \mu_m & \cdots & P_{l-1}(\mu_m), & P_n(\mu_m), & P_{l+1}(\mu_m), & \cdots & P_n(\mu_m) \end{bmatrix}}{\begin{bmatrix} 1 & \mu_0 & \cdots & P_{l-1}(\mu_0), & P_l(\mu_0), & P_{l+1}(\mu_0), & \cdots & P_m(\mu_0) \\ 1 & \mu_1 & \cdots & P_{l-1}(\mu_1), & P_l(\mu_1), & P_{l+1}(\mu_1), & \cdots & P_m(\mu_1) \\ \vdots & \vdots & & \vdots & \vdots & \vdots & & \vdots \\ 1 & \mu_m & \cdots & P_{l-1}(\mu_m), & P_l(\mu_m), & P_{l+1}(\mu_m), & \cdots & P_m(\mu_m) \end{bmatrix}}\ . \tag{35}$$

Paying attention to the following relation:

$$D_{nl}=\begin{cases} 0, & n\neq l,\quad n\leq m \\ 1, & n=l \end{cases}$$

we have

$$S_l(t,x)=-\frac{\alpha d_l}{t(t+\alpha)}A_l(t,x)-\sum_{n=m+1}^{\infty}\frac{\alpha d_n}{t(t+\alpha)}D_{nl}A_n(t,x)\ . \tag{36}$$

Here, μ_i $(i=0,1,\ldots,m)$ is a set of $m+1$ different large-angle directional cosine that are selected arbitrarily to some extent. If the straightforward electrons undergo large elastic or inelastic scattering they will be removed from the straightforward-electron group. They are treated as a source of the diffusion electrons. Thus the small-angle property of the straightforward-electron group remains unchanged. In this case the concept of "mean electron track" can be applied. We introduce an average directional cosine for the straightforward electrons:

$$\mu_a=\int_{-1}^{1}\int_{-1}^{1}f_s(x,\mu,t)\mu d\mu\,dx\Big/\int_{-1}^{1}\int_{-1}^{1}f_s(x,\mu,t)d\mu\,dx=\int_{-1}^{1}A_1(t,x)dx\Big/\int_{-1}^{1}A_0(t,x)dx\ . \tag{37}$$

Integrating the Eq. (24) from $x=-1$ to $x=1$, we have

$$-\frac{d\alpha_l}{dt}=\begin{cases} \displaystyle\sum_{n=m+1}^{\infty}\frac{\alpha d_n}{t(t+\alpha)}D_{nl}\alpha_n+\delta(t), & l\leq m \\ \displaystyle-\frac{\alpha d_l}{t(t+\alpha)}\alpha_l+\delta(t), & l>m\ . \end{cases} \tag{38}$$

Here, α_l is

$$\alpha_l(t)=\int_{-1}^{1}A_l(t,x)dx\ . \tag{39}$$

Using the initial condition

$$f_s(x,\mu,t)\,|_{\,t=1}=\frac{1}{2\pi}\delta(x)\delta(1-\mu)\ , \tag{40}$$

then we have

$$A_l(t,x)\,|_{t=1}=\int_{-1}^{1}\delta(x)\delta(1-\mu)P_l(\mu)d\mu=\delta(x) \tag{41}$$

and

$$\alpha_l(t)\,|_{t=1}=1\ .$$

Thus,

$$\alpha_l(t)=\begin{cases}[t(1+\alpha)/(t+\alpha)]^{d_l}, & l>m\\ -\sum\limits_{n=m+1}^{\infty}D_{nl}\alpha_n(t)+1+\gamma_l, & l\le m\ .\end{cases} \tag{42}$$

From the initial condition

$$\gamma_l=\sum_{n=m+1}^{\infty}D_{nl}=\frac{1}{2l+1}\frac{\begin{bmatrix}1 & \mu_0 & \cdots & \sum\limits_{n=m+1}^{\infty}(2n+1) & P_n(\mu_0), & P_{l+1}(\mu_0), & \cdots & P_m(\mu_0)\\ 1 & \mu_1 & \cdots & \sum\limits_{n=m+1}^{\infty}(2n+1) & P_n(\mu_1), & P_{l+1}(\mu_1), & \cdots & P_m(\mu_1)\\ \vdots & \vdots & & \vdots & & \vdots & & \vdots\\ 1 & \mu_m & \cdots & \sum\limits_{n=m+1}^{\infty}(2n+1) & P_n(\mu_m), & P_{l+1}(\mu_m), & \cdots & P_m(\mu_m)\end{bmatrix}}{\begin{bmatrix}1 & \mu_0 & \cdots & P_l(\mu_0), & P_{l+1}(\mu_0), & \cdots & P_m(\mu_0)\\ 1 & \mu_1 & \cdots & P_l(\mu_1), & P_{l+1}(\mu_1), & \cdots & P_m(\mu_1)\\ \vdots & \vdots & & \vdots & \vdots & & \vdots\\ 1 & \mu_m & \cdots & P_l(\mu_m), & P_{l+1}(\mu_m), & \cdots & P_m(\mu_m)\end{bmatrix}}\ .$$

Expanding the δ function into the Legendre series, we have

$$\delta(\mu-\mu_i)=\sum_{n=0}^{\infty}\frac{(2n+1)}{2}P_n(\mu)P_n(\mu_i)\ .$$

Setting $\mu=1$, then

$$\sum_{n=m+1}^{\infty}(2n+1)P_n(\mu_i)=-\sum_{n=0}^{m}(2n+1)P_n(\mu_i)\ ,$$

therefore

$$\gamma_l=-\sum_{n=0}^{m}D_{nl}=-1$$

and

$$\alpha_l(t)=-\sum_{n=m+1}^{\infty}D_{nl}\alpha_n(t),\quad l\le m\ . \tag{42'}$$

So the mean directional cosine, μ_a, becomes

$$\mu_a=\alpha_1(t)/\alpha_0(t)\ . \tag{43}$$

In order to solve the transport equation of the straightforward electrons approximately, we use the mean directional cosine μ_a instead of the actual directional cosine. Thus, the Eq. (24) becomes

$$-\frac{\partial f_s(x,\mu,t)}{\partial t}+\mu_a\frac{\partial f_s(x,\mu,t)}{\partial x}=C_f-S_{\text{diff}}+\frac{1}{2\pi}\delta(1-\mu)\delta(1-t)\delta(x) \tag{44}$$

or

$$-\frac{\partial A_l(x,t)}{\partial t}+\mu_a\frac{\partial A_l(x,t)}{\partial x}=\begin{cases}-\dfrac{\alpha d_l}{t(t+\alpha)}A_l(x,t)+\delta(1-t)\delta(x), & l>m \qquad (45)\\ \sum\limits_{n=m+1}^{\infty}\dfrac{\alpha d_n}{t(t+\alpha)}D_{nl}A_n(x,t)+\delta(1-t)\delta(x), & l\le m\ . \qquad (46)\end{cases}$$

Using Fourier transformation

$$B_l(p,t)=\int_{-\infty}^{\infty}A_l(x,t)e^{ipx}dx\ , \tag{47}$$

$$A_l(x,t)=\frac{1}{2\pi}\int_{-\infty}^{\infty}B_l(p,t)e^{-ipx}dp\ , \tag{48}$$

we have

$$-\frac{dB_l(p,t)}{dt}-ip\mu_a B_l(p,t)=-\frac{\alpha d_l}{t(t+\alpha)}B_l(p,t)+\delta(1-t),\quad l>m \tag{49}$$

$$B_l(p,t)=[t(1+\alpha)/(t+\alpha)]^{d_l}\exp(ip\int_t^1\mu_a(t')dt'),\quad l>m \tag{50}$$

$$A_l(x,t)=\begin{cases}\left[\frac{t(1+\alpha)}{(t+\alpha)}\right]^{d_l}\delta\left[x-\int_t^1\mu_a(t')dt'\right], & l>m \quad (51)\\ -\delta\left[x-\int_t^1\mu_a(t')dt'\right]\sum_{n=m+1}^{\infty}D_{nl}\left[\frac{t(1+\alpha)}{t+\alpha}\right]^{d_n}, & l\le m \quad (52)\end{cases}$$

$$S_l(x,t)=\delta\left[x-\int_t^1\mu_a(t')dt'\right]\sum_{n=m+1}^{\infty}\frac{\alpha(d_l-d_n)}{t(t+\alpha)}D_{nl}\left[\frac{t(1+\alpha)}{t+\alpha}\right]^{d_n},\quad l\le m\ . \tag{53}$$

For solving the transport equations of the diffusion electrons, the Pn approximation is applicable. Expanding $f_d(x,\mu,t)$ into a series of Legendre polynomials, we have

$$-\frac{\partial N_l(x,t)}{\partial t}+\frac{1}{2l+1}\left[(l+1)\frac{\partial N_{l+1}(x,t)}{\partial x}+l\frac{\partial N_{l-1}(x,t)}{\partial x}\right]=-\frac{\alpha d_l}{t(t+\alpha)}N_l(x,t)+S_l(x,t)\ ;$$

$$l=0,1,\ldots,n;\quad N_{n+1}=0\ . \tag{54}$$

The initial and boundary conditions are

$$N_l(x,t)\,|_{t=1}=0,\quad N_l(x,t)\,|_{x=\pm1}=0\quad (l=0,1,\ldots,n)\ . \tag{55}$$

The Lax-Wendroff scheme has been used for solving Eq. (54).[39] It is convenient to rewrite Eq. (54) into a symmetrical form for using this scheme. Let $M_l(x,t)=(2l+1)^{1/2}N_l(x,t)$. Thus, we have

$$-\frac{\partial M_l(x,t)}{\partial t}=-\frac{l+1}{(2l+1)^{1/2}(2l+3)^{1/2}}\frac{\partial M_{l+1}(x,t)}{\partial x}-\frac{l}{(2l-1)^{1/2}(2l+1)^{1/2}}\frac{\partial M_{l-1}(x,t)}{\partial x}-\frac{\alpha d_l}{t(t+\alpha)}M_l(x,t)+\sqrt{2l+1}S_l(x,t) \tag{56}$$

and

$$M_l(x,t)\,|_{t=1}=0,\quad M_l(x,t)\,|_{x=\pm1}=0\quad (l=0,1,\ldots,n)\ . \tag{57}$$

Using the Lax-Wendroff discrete scheme, one obtains a numerical solution of Eq. (56).

The energy deposition of electrons in a medium is

$$D_E(x)=\int_0^1[A_0(x,t)+N_0(x,t)]\frac{dE}{dt}dt\ . \tag{58}$$

Paying attention to the relation

$$A_0(x,t)=\delta\left[x-\int_t^1\mu_a(t')dt'\right]\alpha_0(t) \tag{59}$$

and assuming τ to satisfy the following equation:

$$x=\int_{\tau(x)}^1\mu_a(t')dt'\ . \tag{60}$$

It leads to

$$\delta\left[x-\int_t^1\mu_a(t')dt'\right]=\delta[\mu_a(\tau)(t-\tau)]\ , \tag{61}$$

$$D_E(x)=\left[\frac{dE}{dt}\right]_{t=\tau}\frac{\alpha_0^2(\tau)}{\alpha_1(\tau)}+\int_0^1 N_0(x,t)\frac{dE}{dt}dt\ . \tag{62}$$

IV. COMPUTATIONAL RESULTS

A. Scope of our calculations

As mentioned above, the purpose of this work is to develop a flexible analytical theory of electron transport. In order to examine the validity of the theory an extensive comparison was made between results obtained by using the bipartition model and those given by Spencer's moment method. When possible, comparison was also made with experimental results. We calculated the energy deposition of electrons of 0.05, 0.1, 0.4, 1, 4, and 10 MeV in carbon, aluminium, copper, tin, the energy deposition of electrons of 0.1, 1, and 10 MeV in air and polystyrene and the energy deposition of electrons of 0.1, 0.7, 1, and 2 MeV in lead. Our calculation scope almost covers that of Spencer. In addition the energy deposition in a cavity filled with air located in aluminum produced by electrons of 2 and 0.1 MeV has been calculated and compared with Trump and Huffman's experimental results.[40] In order to compare our results with Grün's experimental data the energy deposition of electrons of 0.025 and 0.05 MeV in air has been calculated, and the energy deposition of electrons with 0.032 MeV in air has been obtained by linear interpolation.

B. Selection of the parameters

The basic parameters involved in the calculation are stopping power and scattering coefficients. For the sake

of comparing our results with those of Spencer, the parameters used in this work are that of Spencer's tables.[41] Spencer gave, however, only 12 scattering coefficients S_l for one medium and one electron energy. This is not sufficient for our calculations. Several tens of scattering coefficients are needed, particularly for the initial stage of penetration, in order to obtain precise results for the fluence of the straightforward electrons. For example, we made use of 80 scattering coefficients for the calculation of the energy deposition of the straightforward electrons in carbon. Therefore it is necessary to extrapolate Spencer's tables. Let S_l be the lth scattering coefficient ($l>12$). The extrapolation formula is

$$S_l = S_{12} C_l / C_{12} \ . \tag{63}$$

Here, C_l is decided by Spencer's recurrent formulas:[26]

$$C_0 = 0 \ , \tag{64}$$

$$C_1 = \ln(1+\eta^{-1}) - (1+\eta)^{-1} \ , \tag{65}$$

$$C_{l+1} = (2+l^{-1})(1+2\eta)C_l - (1+l^{-1})C_{l-1} - (2l+l^{-1})(1+\eta)^{-1} \ . \tag{66}$$

When calculating the coefficients C_l, the relativistic effect has not been taken into account, because this effect has already been considered in the first 12 scattering coefficients. Furthermore, with increasing l, the importance of the relativistic effect decreases remarkably. For the sake of simplicity it has been neglected.

The specified directional cosines μ_i for the partition condition are selected arbitrarily to some extent. Choosing different μ_i influences the computational results only a little, as shown in Fig. 2.

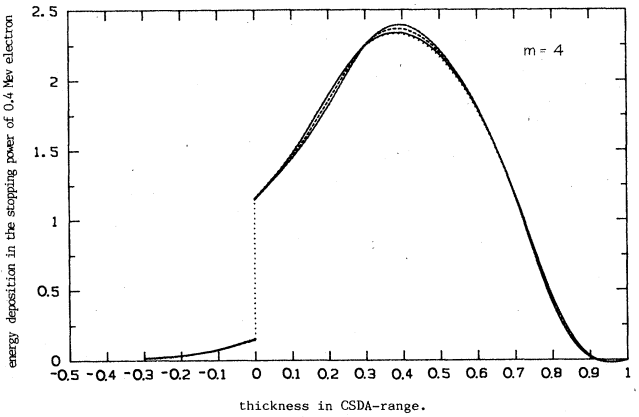

FIG. 2. Influence of different sets, of which every one consists of five large-angle directional cosines chosen arbitrarily, on the calculation of the energy deposition produced by 0.4-MeV electron in carbon: —— (−1, −0.866, −0.5, 0, 0.5), · · · · (−1, −0.6, −0.2, 0.2, 0.6), ——— (−1, −0.7, −0.4, −0.1, 0.2), and — — — (−1, −0.75, −0.5, −0.25, 0).

C. Numerical method

The Lax-Wendroff scheme is one of most effective numerical methods for solving hyperbolic partial differential equations. Therefore, it has been used here for solving the transport equations of the diffusion electrons. The symmetrical matrix expression of the transport equation of the diffusion electrons under the Pn approximation is

$$-\frac{\partial \tilde{\mathbf{N}}}{\partial t} = A\frac{\partial \tilde{\mathbf{N}}}{\partial x} + B\tilde{\mathbf{N}} + \tilde{\mathbf{S}} \ , \tag{67}$$

where

$$\tilde{\mathbf{N}} = \begin{bmatrix} \tilde{N}_0 \\ \tilde{N}_1 \\ \vdots \\ \tilde{N}_n \end{bmatrix}, \quad \tilde{\mathbf{S}} = \begin{bmatrix} S_0 \\ \sqrt{3}S_1 \\ \vdots \\ \sqrt{2m+1}S_m \\ 0 \\ \vdots \\ 0 \end{bmatrix}, \quad A = \begin{bmatrix} 0 & \frac{1}{\sqrt{3}} & & & 0 \\ \frac{1}{\sqrt{3}} & 0 & & & \\ & & \ddots & & \\ & & & & \frac{1}{\sqrt{(2n-1)(2n+1)}} \\ 0 & & & \frac{1}{\sqrt{(2n-1)(2n+1)}} & 0 \end{bmatrix}, \tag{68}$$

$$B = \begin{bmatrix} 0 & & & \\ & \frac{\alpha d_1}{t(t+\alpha)} & & 0 \\ & & \ddots & \\ 0 & & & \frac{\alpha d_n}{(t+\alpha)} \end{bmatrix}, \quad \tilde{N}_l = (2l+1)^{1/2} N_l \ .$$

The Lax-Wendroff scheme of second-order accuracy can be written in a recurrent form:[39]

$$\tilde{N}_{\mu}^{i+1,j}=\left[\tilde{N}_{\mu}^{i,j}+\frac{p}{2}A_{\mu\nu}(\tilde{N}_{\nu}^{i,j-1}-\tilde{N}_{\nu}^{i,j+1})+\frac{p^2}{2}A_{\mu\nu}^2(\tilde{N}_{\nu}^{i,j+1}-2\tilde{N}_{\nu}^{i,j}+\tilde{N}_{\nu}^{i,j-1})\right.$$
$$\left.-\Delta tB_{\mu}^{i}\delta_{\mu\nu}\tilde{N}_{\nu}^{i,j}/2-\Delta t(\tilde{S}_{\mu}^{i+1,j}+\tilde{S}_{\mu}^{i,j})/2\right]\Big/(1+\Delta tB_{\mu}^{i+1}/2)\,. \tag{69}$$

i and j in Eq. (69) express the ith and jth nodes along the t and x axis, respectively, and repeated greek subscripts means summation. The order n of the Pn approximation has certain influence on the calculational results, but when $n \geq 5$, the influence is not significant (as shown in Fig. 3).

The influence of the number of nodes on the calculation is shown in Fig. 4. The interval $(-1,1)$ has been divided into 400, 200, 160, and 80 segments respectively. Then the energy deposition of electrons of 0.4 MeV in aluminium was calculated. The computational results show no significant difference. Therefore, the pattern of 200 segments was frequently used in our calculations.

D. Comparison with other theories and experiments

In Figs. 5–9 the energy deposition of 1-MeV electrons in carbon, aluminium, copper, tin, and lead are, respectively, given together with Spencer's results. Table I shows the mean-square-root deviation between our calculations and those of Spencer. The deviation is defined as

$$\Delta=\left[\int_{-1}^{1}[D_E(x)-D_s(x)]^2dx\Big/\int_{-1}^{1}D_E^2(x)dx\right]^{1/2}, \tag{70}$$

where the $D_s(x)$ are taken from Spencer's tables. It can be seen from these figures and Table I that the two theories are in good agreement. Particularly, there is only a small difference for the energy deposition in the deep penetration region. The positions and the values of the maximum energy deposition agree well also. Compared with some experiments, especially with those of Grün's measurements,[29] we have found that the precision of our results are comparable to those of Spencer's moment method. In Fig. 10 the energy deposition curve of 0.032-MeV electrons in air obtained by interpolation is compared with Grün's experiments. It shows that the results of the bipartition model are very good. As well, from Fig. 11 the agreement between our results and Huffman's measurement is also good.

It should be pointed out that the systematic deviations between the bipartition model and the moment method cannot be neglected, although they are not large compared to the accuracy of the measurements. The systematic deviations occur mainly in the vicinity of the source plane. Although the experimental data in this region generally seem to favor our results, it is too early to draw a conclusion. In addition, it is known that the description of the backscattering is a shortcoming of Spencer's theory. Naturally the description of the backscattering could influence the calculation of the energy deposition in the initial stage of the electron penetration to some extent. Moreover, the stopping power formula given by using a numerical fitting technique is not suitable for a numerical differentiation. Otherwise, the precision of the deviation of the fitted stopping power formula would be reduced significantly.

We now compare the computational efficiencies of the bipartition model to that of the Monte Carlo method. The computational time spent by the bipartition model is much less than that spent by the Monte Carlo method for the same calculation of electron transport. For most of

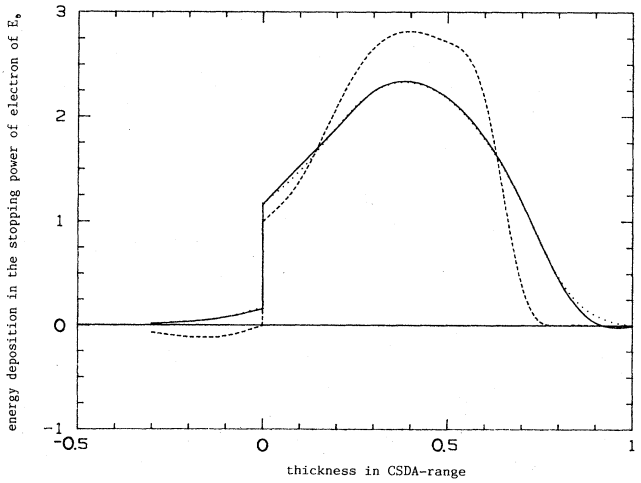

FIG. 3. Influence of the Pn approximations of different orders on the calculation of the energy deposition produced by 0.4-MeV electron in carbon: ——, $n=11$; · · · ·, $n=3$; and ——, $n=1$.

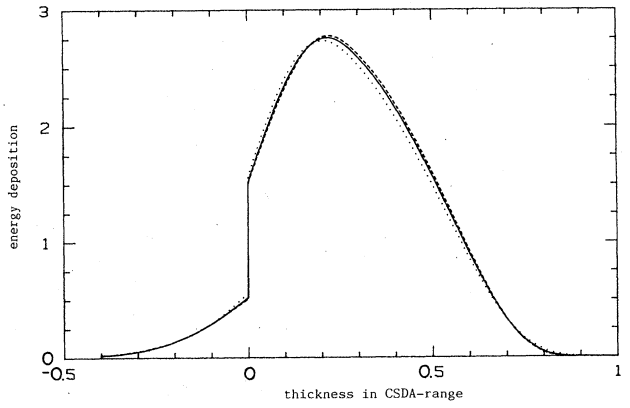

FIG. 4. Influence of the different numbers of nodes on the calculation of the energy deposition produced by 0.4-MeV electron in aluminium: ——, $N=200$; ——, $N=400$; and · · · ·, $N=80$.

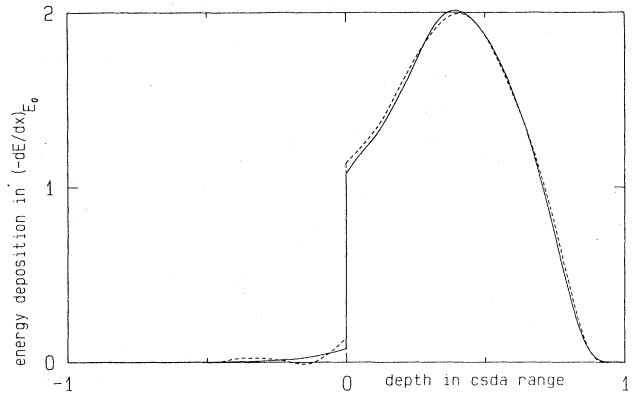

FIG. 5. Energy deposition produced by 1-MeV electron in carbon. Solid line is our result. Dashed line is Spencer's result.

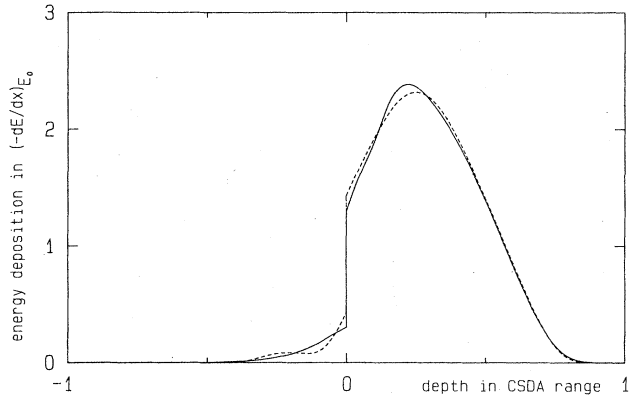

FIG. 6. Energy deposition produced by 1-MeV electron in aluminium. Solid line is our result. Dashed line is Spencer's result.

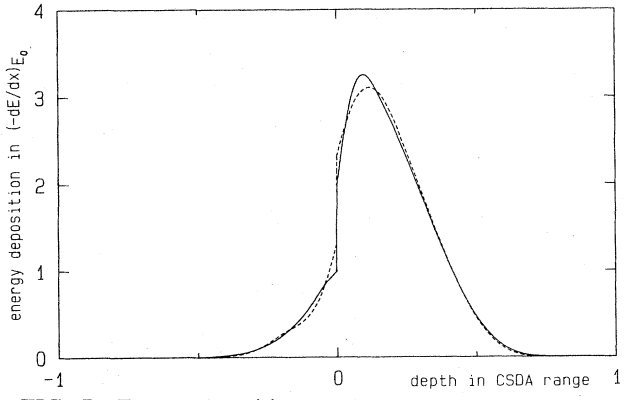

FIG. 7. Energy deposition produced by 1-MeV electron in copper. Solid line is our result. Dashed line is Spencer's result.

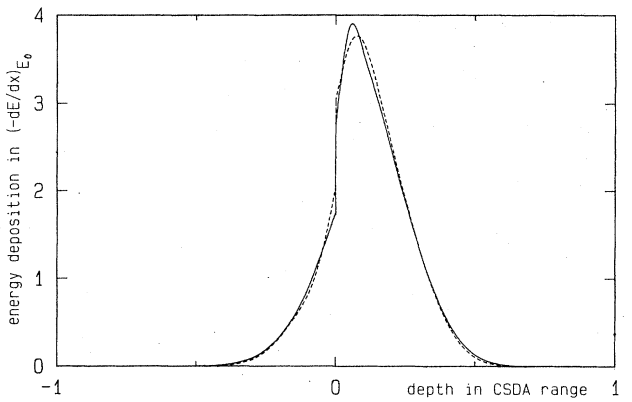

FIG. 8. Energy deposition produced by 1-MeV electron in tin. Solid line is our result. Dashed line is Spencer's result.

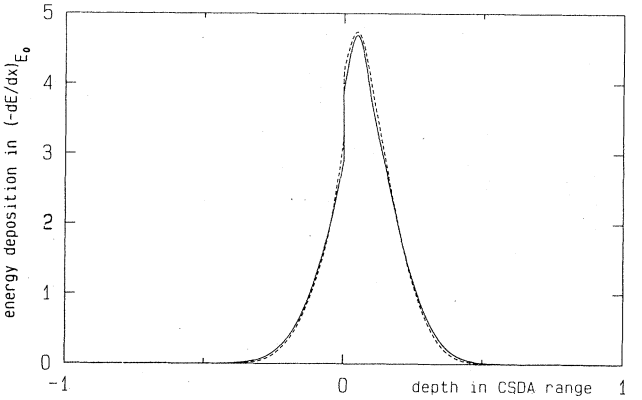

FIG. 9. Energy deposition produced by 1-MeV electron in lead. Solid line is our result. Dashed line is Spencer's result.

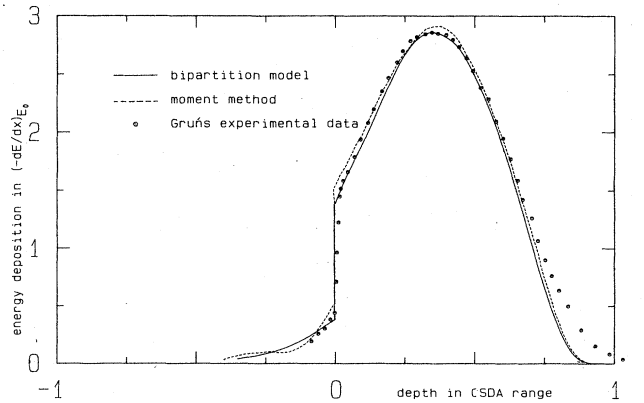

FIG. 10. Comparison among results obtained by the bipartition model, Spencer's moment method, and Grün's experimental data for 32-keV electron.

TABLE I. A comparison between Spencer's moment method and bipartition model. Δ is the average square-root deviation of electron-energy deposition.

	Δ		
	0.1 MeV	1 MeV	10 MeV
Carbon	0.021	0.023	0.026
Aluminium	0.028	0.030	0.020
Copper	0.038	0.048	0.018
Tin	0.033	0.050	0.058
Lead	0.028	0.042	
Polystyrene	0.014	0.015	0.022
Air	0.022	0.020	0.032

TABLE II. Dependence of T_c upon n and N.

	n			
N	1	3	5	7
80		23		45
160		87		173
200	63	136	206	268

the computational examples presented here the standard parameters are chosen as $m=4$, $n=7$, and $N=200$. In this case the computational time needed is about 270 sec for obtaining most transport quantities of interest, such as, the electron-energy deposition, the electron flux and the current, the angular distribution, the energy spectrum, and the range distribution. Our computer executes about 10^6 elementary operations per second. It should be pointed out that the computational time, T_c, strongly depends on the parameters n and N, i.e., $T_c \alpha n N^2$. Table II gives the values of T_c for various choices of the parameters. It should be emphasized that the computational precision will weakly depend on the parameters n and N, if $n \geq 3$ and $N \geq 80$. The calculation has shown the computational time to be reduced from 270 to 25 secs for a transport calculation without obvious change in the precision. Therefore, the bipartition model shows a potential of the application to the cases where the Monte Carlo is limited.

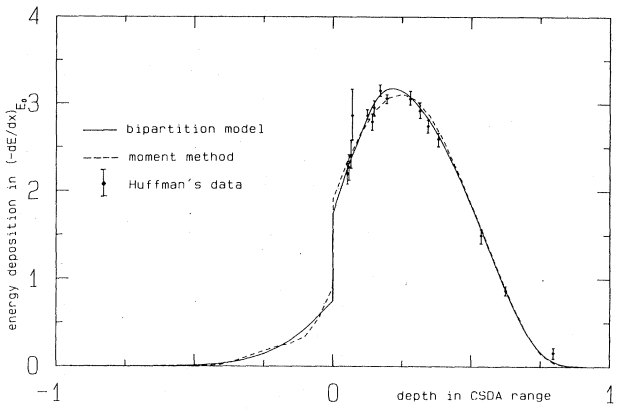

FIG. 11. A comparison among results obtained by the bipartition model, Spencer's moment method, and Huffman's experiments for 0.1-MeV electron.

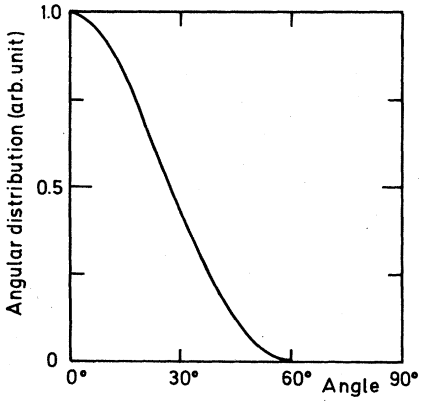

FIG. 12. Demonstration of the angular distribution of the straightforward electrons.

E. Assessment of the small-angle property of the straightforward electrons

It is necessary to assess the approximation of using the average directional cosine instead of the actual directional cosine. The average directional cosine of the straightforward electrons at the different thickness have been given

TABLE III. Dependence of the average directional cosine upon the thickness x.

	$x=$	0.00	0.10	0.20	0.30	0.40	0.50	0.60	0.70	0.80	0.90
C	0.1 MeV	1.000	0.931	0.880	0.853	0.841	0.834	0.831	0.829	0.829	0.828
	10 MeV	1.000	0.983	0.956	0.929	0.898	0.871	0.851	0.839	0.831	0.829
Al	0.1 MeV	1.000	0.885	0.846	0.835	0.830	0.829	0.829	0.828	0.828	0.828
	10 MeV	1.000	0.958	0.918	0.880	0.854	0.840	0.833	0.830	0.829	0.828
Cu	0.1 MeV	1.000	0.847	0.831	0.829	0.828	0.828	0.828	0.828	0.828	0.282
	10 MeV	1.000	0.911	0.857	0.839	0.832	0.829	0.828	0.828	0.828	0.828
Pb	0.1 MeV	1.000	0.872	0.841	0.835	0.834	0.834	0.834	0.834	0.834	0.834
	10 MeV	1.000	0.842	0.835	0.834	0.834	0.834	0.834	0.834	0.834	0.834

in the Table III. It would be interesting that the stationary angular distribution of the straightforward electrons can be found after a short penetration distance. As an example, the angular distribution of the straightforward electrons of 0.4 MeV initial energy at $x=0.3$ in aluminium is shown in Fig. 12. The corresponding angular mean square root of the deviation $\langle\delta\theta\rangle$ is about 11°. By definition $\langle\delta\theta\rangle$ is

$$\langle\delta\theta\rangle=\left[\int_0^{\pi}\int_0^1 f_s(x,\mu,t)(\theta-\bar{\theta})^2\sin\theta\,d\theta\,dt\Big/\int_0^{\pi}\int_0^1 f_s(x,\mu,t)\sin\theta\,d\theta\,dt\right]^{1/2},$$

$$\bar{\theta}=\int_0^{\pi}\int_0^1 f_s(x,\mu,t)\theta\sin\theta\,d\theta\,dt\Big/\int_0^{\pi}\int_0^1 f_s(x,\mu,t)\sin\theta\,d\theta\,dt\ .$$

Therefore, it is reasonable to utilize the average directional cosine instead of the actual one.

We come to the following conclusion: The bipartition model shows high accuracy. The systematic deviation between the bipartition model and the moment method needs to be further verified with more precise experiments and more accurate data on the interaction between electron and matter. In the next part of our work the bipartition model will be applied to a practically important case which the other analytical theories have hardly treated, the transport of electrons in inhomogeneous media.

ACKNOWLEDGMENTS

The author would like to express his sincere thanks to Professor A. M. Kellerer for his support and his instructive discussions on this work, and to Lassmann, Friede, Schüllner, and Mäder for their help in the numerical calculations. This work is part of the research program submitted by the author to the Alexander von Humboldt Foundation, to which the author is very grateful for its finanical support.

*Permanent address: North China Institute of Radiation Protection, P.O. Box 120, Tai Yuan, Shanxi, People's Republic of China.

[1]Luo Zheng-ming, Radiat. Res. **92**, 1 (1982); *A Theory of Electron Multiple Scattering and Electron Energy Losses,* in *Collected Papers in Atomic Energy and Technology* (Atomic Energy Press, Beijing, 1976) (in Chinese).
[2]J. E. Leiss, Phys. Rev. **107**, 1544 (1957).
[3]M. J. Berger, *Monte-Carlo Calculation of the Penetration and Diffusion of Fast Charged Particles,* in *Methods in Computational Physics,* edited by B. Alder, S. Fernbach, and M. Rotenberg (Academic, New York, 1963), Vol. 1.
[4]M. J. Berger and S. M. Seltzer, National Bureau of Standards Report No. NBSIR-82-2451 (1982) (unpublished).
[5]M. J. Berger and S. M. Seltzer, National Aeronautics and Space Administration Report No. NASA-SP-169 (1968) (unpublished).
[6]M. Kneidler and J. Silverman, International Atomic Energy Agency Report No. IAEA-STI/PUB/236,567-576, Vienna (1969) (unpublished).
[7]M. Green, Proc. Phys. Soc. **82**, 204 (1963).
[8]H. E. Bishop, Proc. Phys. Soc. **85**, 855 (1965).
[9]C. K. Chen *et al.*, Appl. Phys. A **31**, 37 (1983).
[10]M. T. Robinson *et al.*, Phys. Rev. B **9**, 5008 (1974).
[11]L. Landau, J. Phys. (U.S.S.R.) **8**, 201 (1944).
[12]O. Blunck and S. Leisegang, Z. Phys. **128**, 500 (1950).
[13]K. R. Symon, thesis, Harvard University, 1948 (unpublished).
[14]P. V. Vavilov, Pis'ma Zh. Eksp. Teor. Fiz. **32**, 920 (1957) [JETP Lett. **5**, 749 (1957)].
[15]T. J. Gooding and R. M. Eisberg, Phys. Rev. **105**, 357 (1957).
[16]E. J. Williams, Proc. R. Soc. London **167**, 531 (1939).
[17]S. Goudsmit and J. L. Saunderson, Phys. Rev. **57**, 24 (1940).
[18]G. Moliere, Z. Naturforsch. **32**, 78 (1948).
[19]H. S. Snyder and W. T. Scott, Phys. Rev. **76**, 220 (1949).
[20]H. A. Bethe, Phys. Rev. **89**, 1256 (1953).
[21]H. W. Lewis, Phys. Rev. **78**, 526 (1950).
[22]C. N. Yang, Phys. Rev. **84**, 599 (1951).
[23]L. A. Kulchitsky and G. D. Latyshev, Phys. Rev. **61**, 254 (1942).
[24]A. O. Hanson *et al.*, Phys. Rev. **84**, 634 (1951).
[25]L. V. Spencer and U. Fano, Phys. Rev. **93**, 1172 (1954).
[26]L. V. Spencer, Phys. Rev. **98**, 1597 (1955).
[27]F. N. Huffman *et al.*, Phys. Rev. **106**, 435 (1957).
[28]I. Adawi, Phys. Rev. **107**, 1476 (1957).
[29]A. E. Grün, Z. Naturforsch. **12a**, 89 (1957).
[30]N. D. Kessaris, Phys. Rev. **145**, 164 (1966).
[31]H. A. Bethe *et al.*, Proc. Am. Philos. Soc. **78**, 573 (1938).
[32]W. Bothe, Z. Phys. **54**, 161 (1929).
[33]J. W. Weymouth, Phys. Rev. **84**, 766 (1951).
[34]W. G. Roesch, Hanford Report No. HW-32121 *Computational Methods in Partial Differential Equations* (Wiley, New York, 1969), p. 169.
[35]M. C. Wang and E. Guth, Phys. Rev. **84**, 1092 (1951).
[36]G. Prillinger, Institut f. Kernenergetik Stuttgart Report No. IKE 6-96 (1977) (unpublished).
[37]Luo Zhengming, Radiat. Res. **84**, 1 (1980).
[38]C. H. Blanchard, Ref. 26.
[39]A. R. Mitchell, *Computational Methods in Partial Differential Equations* (Wiley, New York, 1969), p. 169.
[40]J. G. Trump *et al.*, J. Appl. Phys. **21**, 345 (1950).
[41]L. V. Spencer, National Bureau of Standards, Report No. Monograph-1 (1959) (unpublished).